International Journal of Fluid Power 5 (2004) No. 1 pp. 37-50

MODELLING OF SPOOL POSITION FEEDBACK SERVOVALVES

Dušan Gordić, Milun Babić and Nebojša Jovičić

University of Kragujevac, Faculty of Mechanical Engineering in Kragujevac, Sestre Janjić 6, 34000 Kragujevac, Serbia and Montenegro
gordic@knez.uis.kg.ac.yu, gordic@ptt.yu

Abstract

Based on a critical review of the previous research and the comprehensive theoretical analysis of all functional parts of two-stage electrohydraulic servovalves with a spool position feedback (a current amplifier, a torque motor, the first and the second stage of hydraulic amplification) a detailed mathematical model of the servovalves was created. The analysis was based on the fundamental laws of electromagnetism, fluid mechanics and general mechanics. The model parameters are physical quantities and the complexity of the model is only limited by the possibility of the correct numerical integration. It includes phenomena and quantities that are of influence on the behaviour of the servovalves, so it can predict their function in a wide range of expected working regimes. Results obtained with the numerical modelling on a personal computer were compared with the appropriate experimental data and the validity of the proposed model was confirmed with satisfactory accuracy.

Keywords: electrohydraulics, spool position feedback servovalves, mathematical model

1 Introduction

For the last forty years, electrohydraulic servovalves are used in hydraulic fluid power systems as sophisticated control components. In spite of their relatively long period of application in electrohydraulic servosystems, all phenomena associated with their function are not completely explained. This is due to facts that a relatively complex mathematical apparatus, which includes many parameters, is needed for describing their function and it is very difficult to precisely quantify values of some physical quantities and constants, which figure in these mathematical expressions.

Written articles about various aspects of servovalves appeared alongside of their development and the beginning of commercial application. One of the most significant references from that period, which is almost the indispensable reference of today's researchers, is (Merritt, 1967). In this book, a general description of electrohydraulic system design was given, and principles of the functioning and the design of spool valves, flapper-nozzle valves, torque motors, etc., were defined.

Basically, two different approaches were used for obtaining linear mathematical models that describe the behaviour of electrohydraulic servovalves. According to the first, the servovalve dynamics is neglected or described with the first-, second- or, even, third-order transfer function, depending on the dynamic characteristics of a system that contains the servovalve. The values of time constants, undamped natural frequencies and damping ratios are calculated from the experimentally determined servovalve frequency characteristics that could be found in catalogues of a manufacturer (Karan et al, 1996). Manufacturers principally propose a third-order model of servovalve and a second-order model for the first stage that is a flapper-nozzle valve (Thayer, 1965).

The second approach implies theoretical or theoretical-experimental modelling and linearization about some characteristic working regime (the most frequently is the null position) in order to obtain linear mathematical models. Nevertheless, certain phenomena or physical quantities that are considered to be of less importance are neglected. Researchers thereby propose higher order models presented in the form of transfer functions or state-space equations (Lee et al, 1996; Schothorst, 1997, Tawfik, 1999).

Although available linear models of electrohydraulic servovalves could give preliminary insight of their operation, they are not able to adequately explain and truly predict the response of servovalves over the wide operating range. A review of the experimental frequency responses that every manufacturer provides with their equipment clearly points out the existence of

This manuscript was received on 12 August 2003 and was accepted after revision for publication on 07 January 2004

non-linearities.

Many authors performed the non-linear analysis of various servovalve types and in this way gave contributions to their better understanding and a more realistic explanation of their behaviour. Still Merritt (1967) explained in detail the effects of some non-linearities on the servovalve behaviour. He described the following phenomena: flow forces on a spool and a flapper, torque motor non-linearities (magnetic hysteresis and saturation), friction forces on the spool valve (dry and viscous), etc. He also defined describing functions of the phenomena. The influence of a radial clearance, round corners and an underlap on servovalve static characteristics was analysed by Shearer (1980). In the paper (Arafa and Rizk, 1987) authors made a special review on torques caused by electromagnetic forces, the deformation of a feedback spring and the deformation of the flapper. The research on flapper-nozzle valves, were performed in papers (Lin and Akers, 1991), (Burrows et al, 1991). A non-linear mathematical model based on physical quantities was developed in (Wang et al, 1995). This model include non-linear relations for the torque motor dynamics and a flow force on the flapper, fluid compressibility, the first stage control volume change due to a spool movement, the first stage leakage, and flow forces. The most significant recently published papers wrote Urata (1999) and (2000), who analysed the torque motor dynamics and the elastic structure dynamics in detail.

These articles usually include experimental verification of established models. However, the method of model parameter identification was not shown in the most of these articles. Only specific and selected parameter values are shown in the majority of these articles whereas these parameter values are hidden in some papers due to proprietary requirements (Wang et al, 1995). In some articles these values were not experimentally determined; instead they were tuned so modelling results fit appropriate, experimentally determined characteristics (Wel, 1992; Svensson, 1993).

The authors of this paper tried to create a comprehensive mathematical model of the most widespread servovalves (electrohydraulic two-stage flow control with a spool position feedback). The model complexity was only limited by the possibility of a correct numerical integration.

2 Theoretical Model

Detailed theoretical analysis of the two-stage electrohydraulic servovalves with the spool position feedback is the first step, which should enable an insight into various physical phenomena that are relevant to their behaviour. For this purpose, fundamental laws of electromagnetism, fluid mechanics and general mechanics were used. The knowledge and results of researchers, who dealt with same or similar problems, were used simultaneously. Thus, the theoretical model includes all physical phenomena and quantities that are expected to be of influence on the behaviour of analysed servovalves. All functional units - an electronic current amplifier (although it is not actually the part of servovalves, but is functionally related to them), the torque motor, the flapper-nozzle valve and the spool valve are considered.

2.1 Electronic Amplifier

Electronic current amplifiers have the output current feedback in order to minimise the influences of torque motor coil resistance and inductance. This way, dynamic characteristics of the amplifier are drastically improved, so the dynamics of a current signal forming compared to the dynamic response of a servovalve could be neglected in most cases (Watton, 1989; Urata and Shinoda, 1999; Schorthorst, 1997). Therefore, it can be written:

$$i^* = \begin{cases} K_a \cdot U, & |K_a \cdot U| \le i_s \\ i_s, & |K_a \cdot U| > i_s \end{cases} \tag{1}$$

For servovalves with electrical feedback, this expression is somewhat different due to the influence of internal feedback electrical signal:

$$i^* = \begin{cases} K_a \cdot (U - K_p \cdot y), & |K_a \cdot (U - K_p \cdot y)| \le i_s \\ i_s, & |K_a \cdot (U - K_p \cdot y)| > i_s \end{cases} \tag{2}$$

2.2 Torque Motor

When current is made to flow through torque motor coils, armature ends become polarised. A torque is thus produced on the armature and it moves. Researchers mostly use a linear expression to calculate this torque:

$$T_e = K_i \cdot i^* + K_m \cdot \theta \tag{3}$$

where values for K_i and K_m that depend on the connection of coils, are obtained experimentally.

Taking into account expressions for electromagnetic forces in torque motor air gaps, where expressions for magnetic fluxes in air gaps (obtained using the first and the second Kirchhoffs' laws for magnetic circuits) are implemented, various expressions are obtained in cases of serial, parallel and push–pull coil connection, that can be generalised into (Gordić, 2002):

$$T_e = \frac{r \cdot \mu_0 \cdot A_p}{x_{p0}^2} \cdot \left(M_m + k_c \cdot N \cdot \frac{r \cdot \theta}{x_{p0}} \cdot i^* \right) \cdot \frac{\left[M_m \cdot \frac{r \cdot \theta}{x_{p0}} + k_c \cdot N \cdot (1 + k_r) \cdot i^* \right]}{\left[1 - \left(\frac{r \cdot \theta}{x_{p0}} \right)^2 + k_r \right]^2} \tag{4}$$

Linearising Eq. 4 about the null position ($i^* = 0$ and $\theta = 0$) one can write:

$$K_i = \frac{k_c \cdot N \cdot r \cdot \mu_0 \cdot A_p \cdot M_m}{x_{p0}^2 \cdot (1 + k_r)} \tag{5}$$

$$K_{\mathrm{m}} = \frac{r^2 \cdot \mu_0 \cdot A_{\mathrm{p}} \cdot M_{\mathrm{m}}^2}{x_{\mathrm{p}0}^3 \cdot (1+k_{\mathrm{r}})^2} \tag{6}$$

Comparing equations for theoretical determination of K_{i} and K_{m} (Merritt, 1967; Schorthorst, 1997) with Eq. 5 and 6, it can be noticed that these expressions have an additional member, in this paper designated as so-called "magnetic reluctance constant" - k_{r}. It considers influences of permanent magnet reluctance, the non-uniformity of a magnetic field through the permanent magnet volume, reduction of the magnetic field in the permanent magnet due to influences of end poles and the leakage flux in air gaps, as it was described in (Urata, 2000). Following expressions should be used for its calculation:

$$k_{\mathrm{r}} = \frac{R_{\mathrm{mm}}}{R_{\mathrm{mp}0}} \cdot \frac{1}{k_{\mathrm{l}}} \tag{7}$$

where

$$R_{\mathrm{mm}} = \frac{l_{\mathrm{m}}}{A_{\mathrm{m}} \cdot \mu_{\mathrm{m}}} \cdot \frac{1}{k_{\mathrm{m}}} \tag{8}$$

$$R_{\mathrm{mp}0} = \frac{x_{\mathrm{p}0}}{\mu_0 \cdot A_{\mathrm{p}}} \tag{9}$$

Computed results for K_{i} and K_{m} are significantly closer to experimental values when considering k_{r}.

2.3 Armature Dynamics

Under the influence of the torque caused by electromagnetic forces, an armature assembly (consisting of the armature and the flapper) moves. In order to cancel the negative influence of the torque motor electromagnetic spring constant, the armature assembly requires a flexure tube as an elastic support. The armature assembly and the flexure tube move and deform together. Although the movement of the armature assembly and the flexure tube is complex, it should be assumed that the armature assembly turns around an axis (Urata, 1999). Applying the law of angular momentum change to armature motion with presumption that the mass of the flexure tube can be neglected since the thickness of its wall is thin the following differential equation could be yield:

$$T_{\mathrm{e}} = \begin{cases} J_{\mathrm{a}} \cdot \ddot{\theta} + k_{\mathrm{v}} \cdot \dot{\theta} + T_{\mathrm{t}} + F_{\mathrm{h}} \cdot l_{\mathrm{a}} + T_{\mathrm{f}}, & |x| < x_0 \\ J_{\mathrm{a}} \cdot \ddot{\theta} + k_{\mathrm{v}} \cdot \dot{\theta} + T_{\mathrm{t}} + F_{\mathrm{h}} \cdot l_{\mathrm{a}} + T_{\mathrm{f}} + T_{\mathrm{i}}, & |x| \geq x_0 \end{cases} \tag{10}$$

Armature motion causes a flexure tube bending. Additional bendable deformation of the flexure tube is caused by the flow force on the flapper (Fig. 1). In order to calculate the torque caused by the flexure tube deformation, it must be presumed that when the flexure tube moves its deflection curve can be approximated by the static one (Urata, 1999; Gordić, 2002). Solving the differential equation of the deflection curve and applying appropriate boundary conditions, equations for the inclination and the deflection of the flexure tube could be obtained. Analysing these equations one can conclude:

1. The armature assembly turns around the axis (point 0 in Fig. 1), which position is:

$$l_{\mathrm{a}} = l_{\mathrm{fl}} - \frac{l_{\mathrm{t}}}{2} \tag{11}$$

2. The torque caused by the flexure tube deformation is:

$$T_{\mathrm{t}} = \frac{B_{\mathrm{t}}}{l_{\mathrm{t}}} \cdot \theta \tag{12}$$

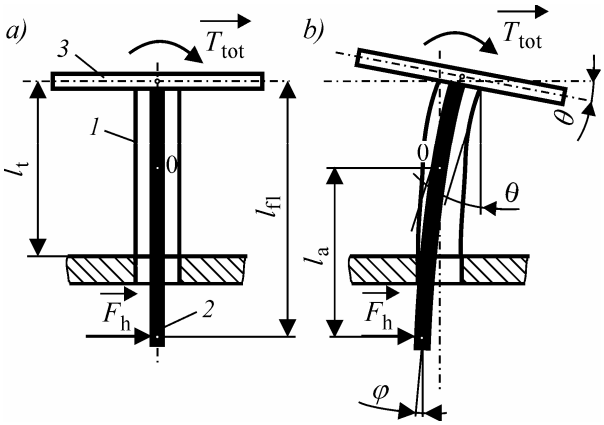

Fig. 1: *Flexure tube and flapper deflection curves a) $\theta = 0$, b) $\theta \neq 0$, 1–flexure tube, 2-flapper, 3-armature*

With the assumption of flapper deflection to the left side, neglecting the influence of flapper tip velocity, the flow force on the flapper is given by (Gordić, 2002):

$$F_{\mathrm{h}} = (p_{\mathrm{l}} - p_{\mathrm{r}}) \cdot \frac{d_{\mathrm{n}}^2 \cdot \pi}{4} + 8 \cdot \pi \cdot \left[K_{\mathrm{nl}}^2 \cdot (x_0 - x)^2 \cdot (p_{\mathrm{l}} - p_{\mathrm{d}}) - K_{\mathrm{nr}}^2 \cdot (x_0 + x)^2 \cdot (p_{\mathrm{r}} - p_{\mathrm{d}}) \right] \tag{13}$$

It is necessary to define the expression for the calculation of a flapper tip displacement in order to implement Eq. 13 into 10. The following equation is obtained using equations for inclinations and deflections of the flexure tube and the flapper, and substituting appropriate boundary conditions (Urata, 1999; Gordić, 2002):

$$x = \theta \cdot l_{\mathrm{a}} - F_{\mathrm{h}} \cdot \left(\frac{l_{\mathrm{fl}}^3}{3 \cdot B_{\mathrm{fl}}} + \frac{l_{\mathrm{t}}^3}{12 \cdot B_{\mathrm{t}}} \right) \tag{14}$$

This equation shows that the flapper tip displacement does not result from the armature motion only, as it is usually considered in analyses.

The torque due to a feedback spring deformation occurs only at servovalves with the mechanical feedback. For its calculation, the following expression should be used (Wel, 1992) (Fig. 2):

$$T_{\mathrm{f}} = F_{\mathrm{f}} \cdot l_{\mathrm{f}} \tag{15}$$

where:

$$F_{\mathrm{f}} = \begin{cases} 0 & |y + y_{\mathrm{ff}}| < z \\ K_{\mathrm{f}} \cdot [y + y_{\mathrm{ff}} - z \cdot \mathrm{sgn}(y + y_{\mathrm{ff}})] & |y + y_{\mathrm{ff}}| \geq z \end{cases} \tag{16}$$

$$y_{\mathrm{ff}} = x + l_{\mathrm{f}} \cdot \varphi \tag{17}$$

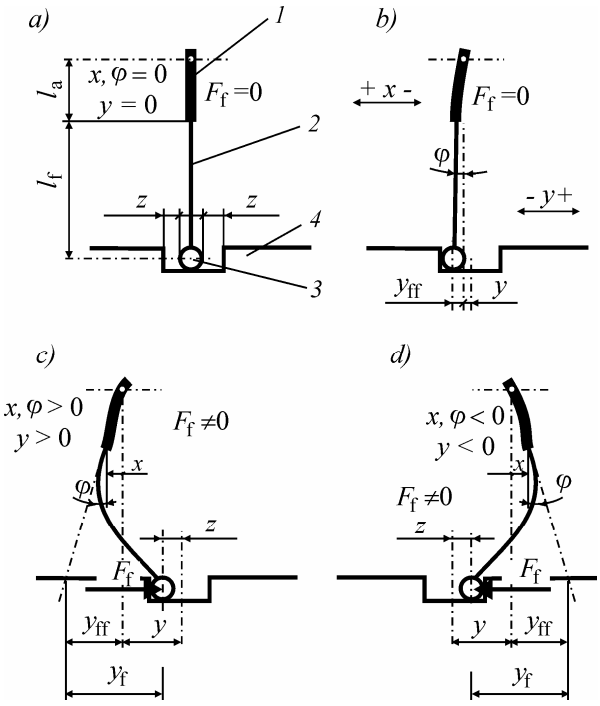

Fig. 2: *Feedback spring/spool interaction a) null position, b) no ball/spool contact, c) and d) ball/spool contact, 1-flapper, 2-feedback spring, 3-ball, 4-spool*

So far, authors considered only $\varphi = \theta$. Due to the influence of the flapper bending, a smaller value for the φ was obtained from the equation of flapper inclination (Gordić, 2002):

$$\varphi = \theta - \frac{F_h \cdot l_{fl}^2}{2 \cdot B_{fl}} \tag{18}$$

It is very hard to quantify the torque exactly due to flapper impact against the tip of a nozzle. Fortunately, these regimes are not of significant importance for the servovalve analysis, because they could be avoided with proper design of servovalve and, especially, servosystem. Therefore, it is not necessary to obtain the value of this torque precisely. However, its value should constrain free armature movement for $|x| \geq x_0$. Considering elastic impact, this torque could be roughly represented as (Vilenius and Vivaldo, 1976):

$$T_i = k_i \cdot (|x| - x_0) \cdot \mathrm{sgn}(x) \cdot l_a \tag{19}$$

2.4 Pressures and Flows in Flapper-Nozzle Valve

Applying the continuity equation to the flapper-nozzle valve, assuming that the flapper tip deflects to the left and the spool moves to the right side[1] (Fig. 3) and neglecting the change of enclosed volumes on each spool side, following equations are obtained:

$$Q_{ol} = Q_{nl} + A_s \cdot \dot{y} + \frac{V_1}{\beta} \cdot \dot{p}_l - \frac{\pi \cdot d_s \cdot \delta^3}{12 \cdot \eta \cdot l_l} \cdot \left(1 + \frac{3}{2} \cdot \left(\frac{e}{\delta}\right)^2\right) \cdot (p_s - p_l) \tag{20}$$

$$Q_{or} = Q_{nr} - A_s \cdot \dot{y} + \frac{V_1}{\beta} \cdot \dot{p}_r - \frac{\pi \cdot d_s \cdot \delta^3}{12 \cdot \eta \cdot l_l} \cdot \left(1 + \frac{3}{2} \cdot \left(\frac{e}{\delta}\right)^2\right) \cdot (p_s - p_r) \tag{21}$$

$$Q_{nl} + Q_{nr} = Q_{od} + \frac{V_d}{\beta} \cdot \dot{p}_d \tag{22}$$

where:
- flows through constant orifices:

$$Q_{ol} = K_{ol} \cdot \frac{d_o^2 \cdot \pi}{4} \cdot \sqrt{\frac{2}{\rho}} \cdot \sqrt{p_s - p_l} \tag{23}$$

$$Q_{or} = K_{or} \cdot \frac{d_o^2 \cdot \pi}{4} \cdot \sqrt{\frac{2}{\rho}} \cdot \sqrt{p_s - p_r} \tag{24}$$

$$Q_{od} = K_{od} \cdot \frac{d_{od}^2 \cdot \pi}{4} \cdot \sqrt{\frac{2}{\rho}} \cdot \sqrt{p_d - p_0} \tag{25}$$

- flows through the nozzles:

$$Q_{nl} = K_{nl} \cdot d_n \cdot \pi \cdot (x_0 - x) \cdot \sqrt{\frac{2}{\rho}} \cdot \sqrt{p_l - p_d} \tag{26}$$

$$Q_{nr} = K_{nr} \cdot d_n \cdot \pi \cdot (x_0 + x) \cdot \sqrt{\frac{2}{\rho}} \cdot \sqrt{p_r - p_d} \tag{27}$$

and the second, the third and the fourth right-hand terms of Eq. 20 and 21 are volumetric flows caused by the spool motion, the fluid compressibility, and the leakage, respectively.

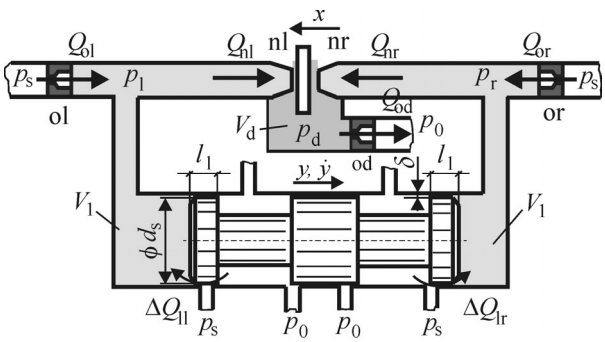

Fig. 3: *Flows and pressures in the flapper-nozzle valve*

Flow coefficients of constant orifices (a short tube type) could be obtained using Lichtarowitz's diagram, Fig. 4-a (McCloy and Martin, 1973), as functions of appropriate Reynolds numbers:

$$Re_{ol} = \frac{d_o}{\nu} \cdot \sqrt{\frac{2}{\rho}} \cdot \sqrt{p_s - p_l} \tag{28}$$

1 For a servovalve with mechanical and electrical feedback. For a servovalve with direct feedback, the spool moves to the opposite side

$$Re_{or} = \frac{d_o}{\nu} \cdot \sqrt{\frac{2}{\rho}} \cdot \sqrt{p_s - p_r} \tag{29}$$

$$Re_{od} = \frac{d_{od}}{\nu} \cdot \sqrt{\frac{2}{\rho}} \cdot \sqrt{p_d - p_0} \tag{30}$$

Flow coefficients of variable flapper-nozzle orifices can be evaluated from the experimentally obtained diagram, Fig. 4-b (Bergada and Codina, 1997), as functions of appropriate Reynolds numbers:

$$Re_{nl} = \frac{2 \cdot (x_0 - x)}{\nu} \sqrt{\frac{2}{\rho}} \cdot \sqrt{p_l - p_d} \tag{31}$$

$$Re_{nr} = \frac{2 \cdot (x_0 + x)}{\nu} \sqrt{\frac{2}{\rho}} \cdot \sqrt{p_r - p_d} \tag{32}$$

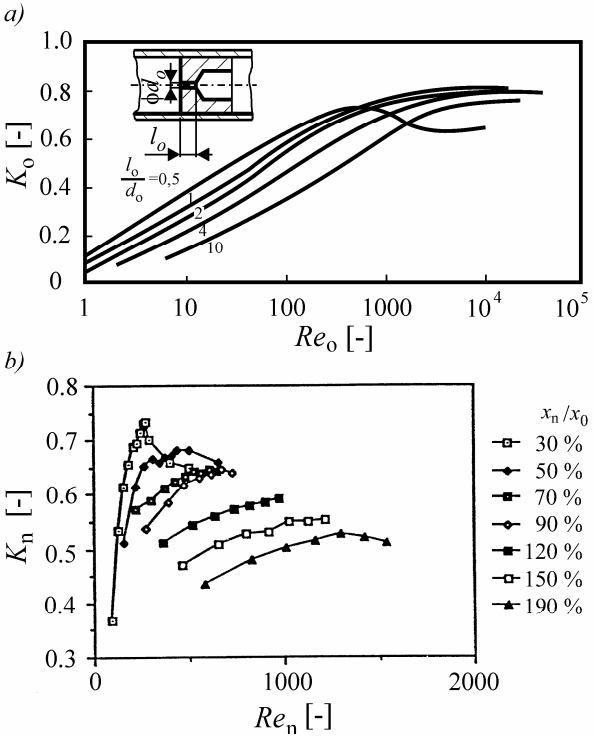

Fig. 4: *Flow coefficients of the first stage a) constant and b) variable orifices (Reproduced from a) (McCloyand Martin, 1973), b) (Bergad and, Codina, 1997))*

Equation 20 - 27 with the application of values from Fig. 4, should enable the calculation of pressures p_l, p_r and p_d. However, implementing the equations into the model, a very complex system of differential equations, which cannot be easily solved, is obtained. The integration of the three pressures and an algebraic loop (necessary for the calculation of the flapper tip displacement - Eq. 14) disables correct numerical solving in the selected software package. Therefore, these equations should be simplified.

Since it was noticed that the greatest obstacle came from the integration of the pressures, it is necessary to neglect terms that include a pressure derivative. Values of these compressibility flows are significantly lower than leakage flows and flows caused by the spool movement, except in the very short starting period of a transient response (Gordić, 2002). In this paper, compressibility flows are neglected in Eq. 20 and 21. Numerical model with complete Eq. 22 and the model where the variation of p_d was neglected, were analysed. A significant difference in output results was not perceived which indirectly confirm the neglect.

Similarly, leakage flows (ΔQ_{ll} and ΔQ_{lr} at Fig. 3) could be neglected (Gordić, 2002).

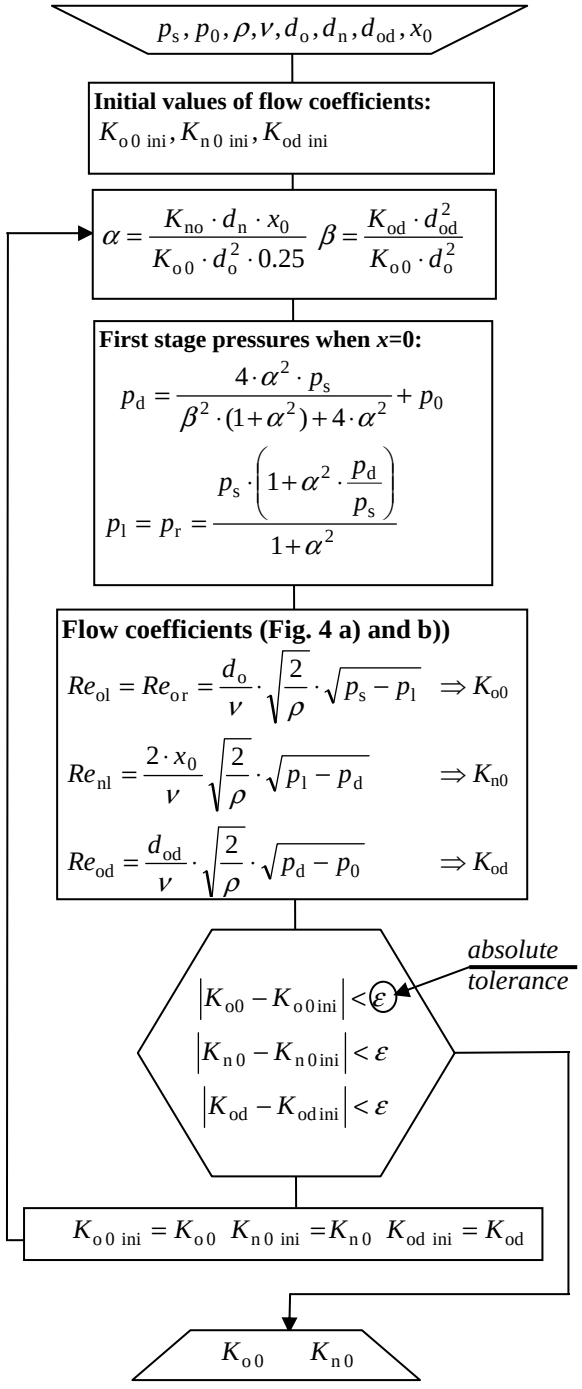

Fig. 5: *Algorithm for the calculation of K_{n0} and K_{o0}*

The third presumption of the simplification is related to the calculation of flow coefficients. It was assumed that flow coefficients of the left and right variable flapper-nozzle orifices are the same and equal to their null value ($K_{nl} = K_{nr} = K_{n0}$). The assumption is

valid for small variations of Reynolds numbers i.e. pressures in the nozzles and the flapper tip displacement. It is not valid in the whole range of flapper tip displacements (Babić et al, 2002), but it cannot be avoided in the numerical integration of servovalve dynamics differential equations. It was also assumed that flow coefficients of left and right constant orifices are the same and equal to their null value ($K_{ol} = K_{or} = K_{o0}$). This assumption is mainly justified (Babić et al, 2002).

Algorithm for the calculation of K_{n0} and K_{o0} is shown in Fig. 5.

After all simplifications Eq. 20 and 21 become:

$$p_l = \frac{a^2 \cdot p_s + b^2 \cdot p_d}{a^2 + b^2} + \frac{d^2 \cdot (b^2 - a^2)}{(a^2 + b^2)^2} - \\ - \frac{2 \cdot a \cdot b \cdot d}{(a^2 + b^2)^2} \cdot \sqrt{(a^2 + b^2) \cdot (p_s - p_d) - d^2} \tag{33}$$

$$p_r = \frac{a^2 \cdot p_s + c^2 \cdot p_d}{a^2 + c^2} + \frac{d^2 \cdot (c^2 - a^2)}{(a^2 + c^2)^2} + \\ + \frac{2 \cdot a \cdot c \cdot d}{(a^2 + c^2)^2} \cdot \sqrt{(a^2 + c^2) \cdot (p_s - p_d) - d^2} \tag{34}$$

where:

$$a = K_{o0} \cdot \frac{d_o^2 \cdot \pi}{4} \cdot \sqrt{\frac{2}{\rho}} \tag{35}$$

$$b = K_{n0} \cdot d_n \cdot \pi \cdot (x_0 - x) \cdot \sqrt{\frac{2}{\rho}} \tag{36}$$

$$c = K_{n0} \cdot d_n \cdot \pi \cdot (x_0 + x) \cdot \sqrt{\frac{2}{\rho}} \tag{37}$$

$$d = A_s \cdot \dot{y} \tag{38}$$

2.5 Spool Dynamics

The differential equation of spool motion can be written as:

$$\Delta p \cdot A_s = m_s \cdot \ddot{y} + k_n \cdot \dot{y} + F_c + F_a + F_f \tag{39}$$

where

$$\Delta p = p_l - p_r \tag{40}$$

A dry (Coulomb) friction force can be mathematically presented as (Southward et al, 1991):

$$F_c = \begin{cases} F_{cn} \cdot \mathrm{sgn}(\dot{y}), & \dot{y} \neq 0 \\ Z, \quad |Z| < F_{c0}, & \dot{y} = 0 \\ F_{c0} \cdot \mathrm{sgn}(Z), \quad |Z| \geq F_{c0}, & \end{cases} \tag{41}$$

where

$$Z = \Delta p \cdot A_s - F_a - (F_f) \tag{42}$$

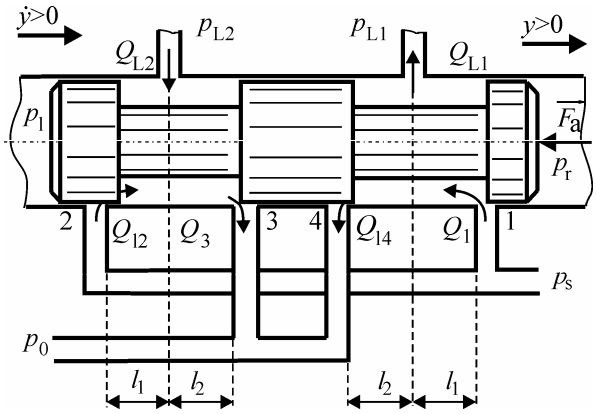

Fig. 6: *A four–way spool servovalve*

The flow force in the spool valve origins from the momentum change in a second stage control volume (Merritt, 1967). In the case of the constant area gradient of the spool valve, which is the most common in a practice, neglecting the influences of members with pressure derivative (Merritt, 1967) and leakage flows, neglecting the time variation of flow coefficients and taking into consideration notations in Fig. 6, the following expression could be used for the axial component of the flow force:

$$F_a = -\sum_{i=1}^{4} (-1)^i \cdot 2 \cdot \frac{K_{ti}^2}{K_{ci}} \cdot f \cdot y_i \cdot \cos\alpha_i \cdot \Delta p_i - \\ - \left(\sum_{i=1}^{2} l_1 \cdot K_{ti} \cdot \sqrt{\Delta p_i} + \sum_{i=3}^{4} l_2 \cdot K_{ti} \cdot \sqrt{\Delta p_i} \right) \cdot \\ \cdot \sqrt{2 \cdot \rho} \cdot f \cdot \dot{y} \tag{43}$$

where the real values of spool valve openings are:

$$y_i = \begin{cases} \sqrt{(\delta + h)^2 + (|j| + h)^2} - h, & y \cdot (-1)^{i+1} \geq -y_{0i} \\ 0, & y \cdot (-1)^{i+1} < -y_{0i} \end{cases} \tag{44}$$

where

$$h = r_s + r_b \tag{45}$$

$$j = y - y_{0i} \cdot (-1)^{i+1} \tag{46}$$

and from Fig. 6:

$$\Delta p_i = \begin{cases} p_s - p_{L1}, & i = 1 \\ p_s - p_{L2}, & i = 2 \\ p_{L2} - p_0, & i = 3 \\ p_{L1} - p_0, & i = 4 \end{cases} \tag{47}$$

Researchers usually use constant values for jet angles α_i=69°, flow coefficients K_{ti}=0.611 and contraction coefficients K_{ci}=0.673, still proposed by Von Mises, when calculating the flow force.

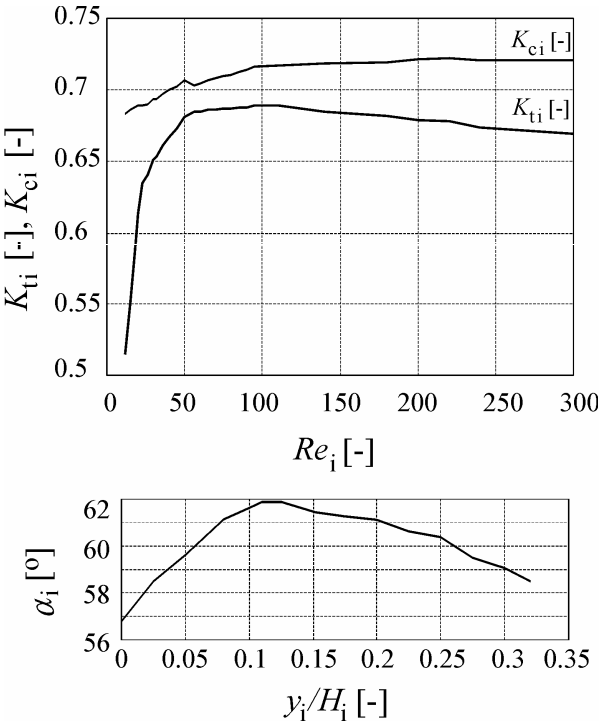

Fig. 7: *Diagrams for the estimation of jet angle, flow coefficient and contraction coefficient (Dong and, Ueno, 1999)*

Numerical data from (Dong and Ueno, 1999) are used in this paper for their calculation (Fig. 7). Diagrammatic data for K_{ti} and K_{ci} are given as functions of Reynolds number, defined with:

$$Re_i = y_i \cdot \sqrt{\frac{2}{\rho}} \cdot \frac{2}{\nu} \cdot \sqrt{\Delta p_i} \tag{48}$$

while the variation of α_i as a function of y_i / H_i ratio with the change of the Re_i is small, so it is neglected. Using these data more correct results for the axial component of the flow force are obtained comparing the results obtained with usual parameter values. (Gordić et al, 2003).

2.6 Spool Control Port Flows

A four-way axial spool servovalve has such a design that flows through its restrictions can be presented by means of a hydraulic bridge. Theoretical, ideal characteristics, that imply the following assumptions: no leakage, matched and symmetrical orifices, a turbulent flow through orifices and the same value of the null lap for all four orifices are derived in (Merritt, 1967), (Watton, 1989). The characteristics analytically describe the fluid flow through spool orifices in the most of working regimes. The exceptions are regimes around the null characterised by an overlap existence when leakages dominate. From the Fig. 6, one can write:

$$Q_{L1} = Q_1 - Q_4 + Q_{l1} - Q_{l4} \tag{49}$$

$$Q_{L2} = Q_3 - Q_2 + Q_{l3} - Q_{l2} \tag{50}$$

where the volumetric flow through i-th spool valve orifice $(i = \overline{1,4})$ is:

$$Q_i = K_{ti} \cdot f \cdot y_i \cdot \sqrt{\frac{2}{\rho}} \cdot \sqrt{\Delta p_i} \tag{51}$$

Several mathematical models for spool valve leakage flows exist (Ellman and Virvalo, 1996), (Ellman, 1998), (Eryilmaz and Wilson, 2000), and their creation implies experimental determination of servovalve static characteristics. Since authors intended to create a model that should be used for servovalve design, they used theoretical model based on the theoretical review in (Mookherjee et al, 2001). This model includes pressure-flow relations for the following orifices: short (based on inflow and outflow along the spool edge), intermediate (based on boundary layer analysis of steady, incompressible developing flow) and long (based on fully developed steady laminar flow through an annular orifice):

$$Q_{li} = \begin{cases} 0, & y \cdot (-1)^i \le -y_{0i} \\ Q_i & y \cdot (-1)^i > -y_{0i} \end{cases} \tag{52}$$

when $\left| y \cdot (-1)^i + y_{0i} \right| < \left(\frac{q}{s} \right)^2 \cdot Q_l$:

$$q \cdot Q_l^2 = \Delta p_i \tag{52-a}$$

when $\left(\frac{q}{s} \right)^2 \cdot Q_l \le \left| y \cdot (-1)^i + y_{0i} \right| < y_{tl}$:

$$s \cdot \left| y \cdot (-1)^i + y_{0i} \right|^{1/2} \cdot Q_l^{3/2} = \Delta p_i \tag{52-b}$$

and when $\left| y \cdot (-1)^i + y_{0i} \right| \ge y_{tl}$:

$$\begin{aligned} & s \cdot y_{tl}^{1/2} \cdot Q_l^{3/2} + \\ & + w \cdot \left(\left| y \cdot (-1)^i + y_{0i} \right| - y_{tl} \right) \cdot Q_l = \Delta p_i \end{aligned} \tag{52-c}$$

where

$$q = \frac{\rho}{2 \cdot K_{ti}^2 \cdot f^2 \cdot \left(\sqrt{(\delta + h)^2 + h^2} - h \right)^2} \tag{53}$$

$$s = \frac{23 \cdot (\rho \cdot \eta)^{1/2}}{f^{3/2} \cdot \delta^{5/2}} \tag{54}$$

$$w = \frac{12 \cdot \eta}{f \cdot \delta^3} \tag{55}$$

A large transition length presents the distance from the entrance at which boundary layers on spool and bushing meet at the mid-plane. It can be obtained as:

$$y_{tl} = \frac{0.075 \cdot \delta \cdot Q_l}{\pi \cdot d_s \cdot \nu} \tag{56}$$

2.7 Interaction with Actuator and Load

The servovalve is used in conjunction with a hydraulic actuator to drive an external load. The servovalve, the actuator, and the load are constantly in

interaction with each other. The purpose of this paper is not to model any component other than the servovalve, but for the calculation of pressures in actuator chambers (p_{L1} and p_{L2}), it is necessary to write additional equations related to the actuator and the load: two continuity equations in actuator chambers and an equation for actuator dynamics. Forms of the equations depend on the electrohydraulic system (type of actuator and load).

All manufactured servovalves are dynamically tested on standard equipment in order to eliminate system influence on their characteristics. In this equipment, the actuator (low mass and low friction double-rod-end cylinder) has no load. Design of the actuator is such that negligible dynamic variations of

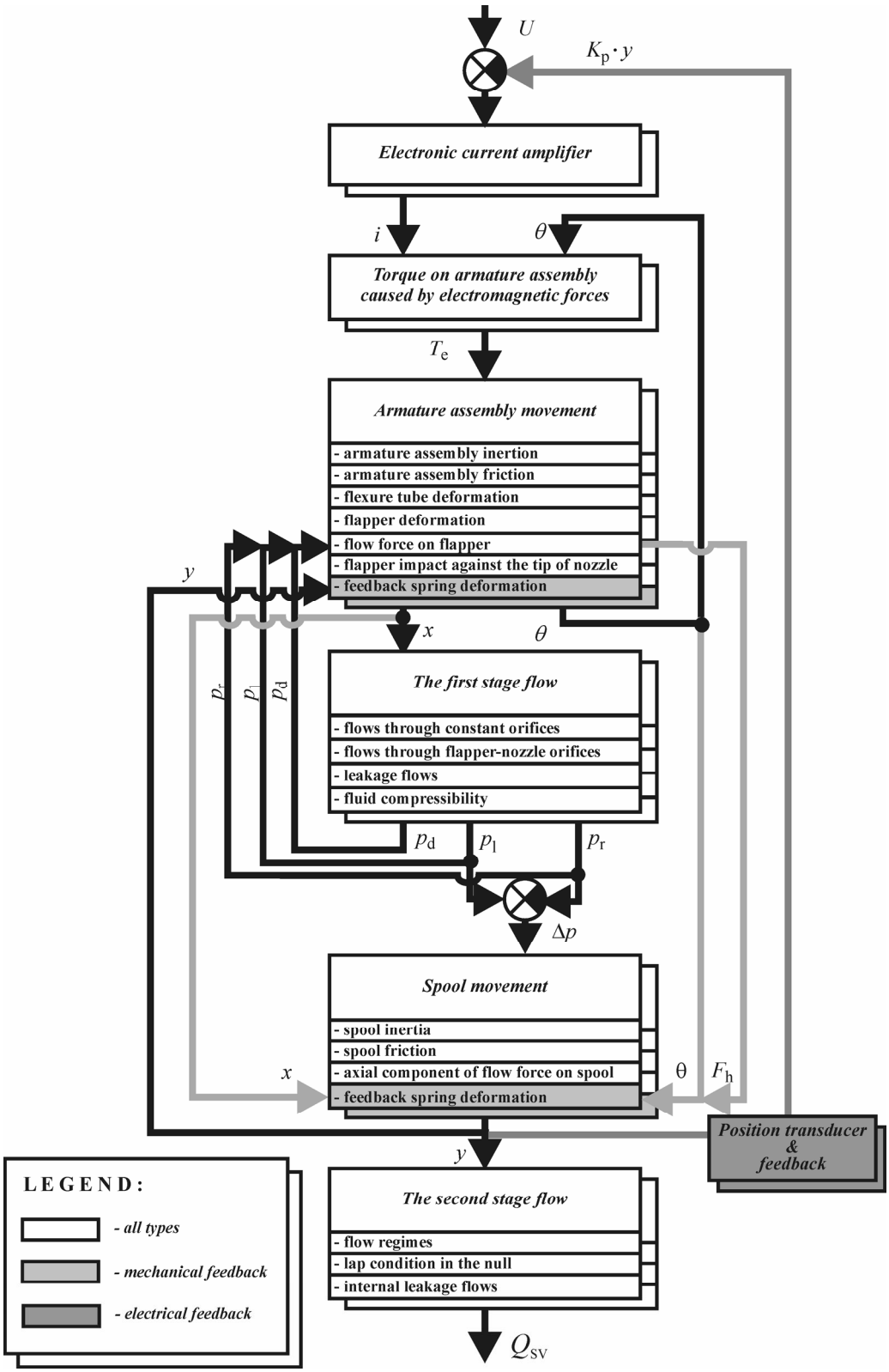

Fig. 8: *The block diagram of no load two-stage electrohydraulic servovalves with the spool position feedback*

pressures in actuator chambers exist in the frequency range of interest. This way, the valve dynamic characteristics in the presence of the true no-load can be ascertained. Therefore, when servovalve has equal lap conditions in all four metering orifices (the most common in the practice) p_{L1} and p_{L2} have constant values:

$$p_{L1} = p_{L2} = \frac{p_s + p_0}{2} \tag{57}$$

If servovalve is analysed separately from the system then only one flow can be used as the output. It is so called the volumetric flow through servovalve, mathematically formulated as:

$$Q_{SV} = \frac{Q_{L1} + Q_{L2}}{2} \tag{58}$$

3 Numerical Model

Taking into account theoretical considerations from the previous chapter, the structural block diagram of the servovalve performance is shown in Fig. 8. Special features of various types of spool position feedback servovalves are emphasised.

The mathematical model for all types of the servovalves could be written using mathematical expressions from the previous chapter. To validate the theoretical review, authors created MATLAB/SIMULINK model of the no-load servovalve with the mechanical feedback using the system of differential Eq. 3, 5-19, 22, 25-58 with diagrams and algorithm from Fig. 4, 5 and 7. Equation 1 was excluded from the model because the current is used as input signal for standard servovalve static and dynamic test procedures.

Table 1: Model parameter values

Symbol	Value	Unit
A_m	154.68	mm^2
A_p	9	mm^2
B_{fl}	0.0256	Nm^2
B_t	0.0302	Nm^2
d_n	0.28	mm
d_o	0.18	mm
d_{od}	0.4	mm
d_s	4.62	mm
e	1	μm
f	2 p. x 2.4	mm
F_{c0}	$(3.04 \div 3.65)\cdot 10^{-3}$	N
F_{cn}	$(1.52 \div 3.04)\cdot 10^{-3}$	N
H_i	1.1	mm
i^*_{max}	10	mA
J_a	$1.68\cdot 10^{-7}$	kgm^2
k_c	1	-
K_f	1962	N/m
k_i	$3\cdot 10^7$	N/m
k_l	0.27	-
k_m	2.42	-
k_n	3800	kg/s
k_r	0.465	-
k_v	$4\cdot 10^{-4}$	Nms
l_1	5.4	mm
l_2	9.2	mm
l_a	8.75	mm
l_{fl}	13	mm
l_l	4.9	mm
l_m	10.9	mm
l_o	0.3	mm
l_{od}	0.4	mm
l_s	13.3	mm
l_t	8.5	mm
M_m	586	A
m_s	3.1	g
N	3625	-
p_0	1	bar
p_s	210	bar
r	14.5	mm
r_b	10	μm
r_s	10	μm
V_1	49.2	mm^3
V_d	8.2	mm^3
x_0	38.5	μm
x_{p0}	0.45	mm
y_{0i}	0	μm
z	2	μm
β	$1.9\cdot 10^9$	Pa
δ	4	μm
η	0.012	Pa·s
μ_m	5	H/m
ν	$14\cdot 10^{-6}$	m^2/s
ρ	871	kg/m^3

The model is numerically solved using parameters of servovalve labelled B.31.210.12.1000.U2V (mechanical feedback) manufactured by PPT – Trstenik, Serbia&Montenegro. Servovalve rate flow is 12 l/min for the input current of 10 mA (the parallel connection of coils) and the oil supply pressure of 210 bar.

Table 1 shows values of quantities and parameters used for numerical modelling.

The manufacturer of permanent magnet provided values of quantities related to permanent magnet except its geometrical quantities, whereas values of constants related to permanent magnet and the torque motor were calculated according to the procedure described in (Urata, 2000).

The interval of possible values of dry friction forces on the spool was estimated based on values of the static and the dynamic friction coefficient for steel/steel contact and the lubricated contact surface, considering the value of the spool mass. This force can be neglected in dynamic analyses because it is much smaller then the force on the spool caused by the difference of nozzle pressures (Gordić, 2002) and the application of a dither signal can diminish it.

Published articles about this subject show that it is practically impossible to precisely determine the viscous friction coefficient of the armature assembly. It can be concluded based on the literature review that the values of this coefficient fall in the wide interval (10^{-4} to 10^0) Nms. It is worth mentioning that in (Hayase et al, 1996), authors used Lamb's equation to obtain the

friction coefficient. The usage of this equation additionally complicates the model because it utilizes a variable speed term.

Similar remarks are valid for the spool viscous friction coefficient because it is also hard to determine its value. Authors propose values from the interval (0 to 4.000) kg/s. Some authors calculate its value using Petroff's law (Yeaple, 1997). The application of this law on the analysed servovalve would result in a value of 0.8 kg/s, which is, although in the proposed interval, inadequate for the correct numerical integration.

In this paper, the friction coefficients were estimated to match the appropriate experimental transient responses. Their values are interrelated. The increase of k_v or the decrease of k_n slows the transient response. The decrease of k_v or the increase of k_n speeds the transient response. The influence of k_n variation on transient response characteristics is bigger because smaller variations of k_n value provokes substantial changes in transient response characteristics. According to their experience, the authors expect that values of k_v should be found within the interval $(2 \text{ to } 10)\cdot 10^{-4}$ Nms, while values of k_n within $(2 \text{ to } 4)\cdot 10^3$ kg/s, when the fluid is mineral oil.

The value for "impact stiffness" is estimated from the lateral rigidity of nozzle tube.

Values for other physical quantities and constants are determined with a direct measurement on the disassembled servovalve. The equilibrium distance from the flapper tip to nozzles is an exception from this rule. It was calculated according to the assemblage requirement, which demands that pressures in both nozzles should be 70 bar when the supply pressure is 140 bar and when the flapper is in the null position.

The numerical analysis was performed implementing several MATLAB variable-step solvers for stiff systems. Results are identical for all cases and solutions practically converge with the same speed.

4 Model Verification

Results of the numerical analysis were compared with appropriate experimental results in order to verify the model. Static and dynamic experimental analyses of B.31.210.12.1000.U2V servovalve were performed on the standard servovalve testing equipment, property of PPT (static - MOOG-PLOTTERSTAND D046-030, dynamic - MOOG-FREQUENZGANG - PREUF-STAND D046032). These experimental stands mainly provide the conditions expressed with Eq. 57 during performed experiments.

Aero Shell Fluid 4 - mineral oil was used as a working fluid. The experiments were performed at the constant ambient temperature of 20°C. The supply pressure was 210 bar in all the cases.

Taking into account the expected dynamic characteristics of the servovalve, the square periodic signal was chosen (frequency was 10 Hz) for dynamical testing. Amplitudes of the input current signal were varied. In Fig. 9, results of numerical and experimental analyses for three input current signals (5%, 10% and 25% of the rated current signal) are comparatively presented. The transient response from the stationary regime determined with the current signal $-i^*$ to the stationary regime determined with the current signal $+i^*$ was analysed.

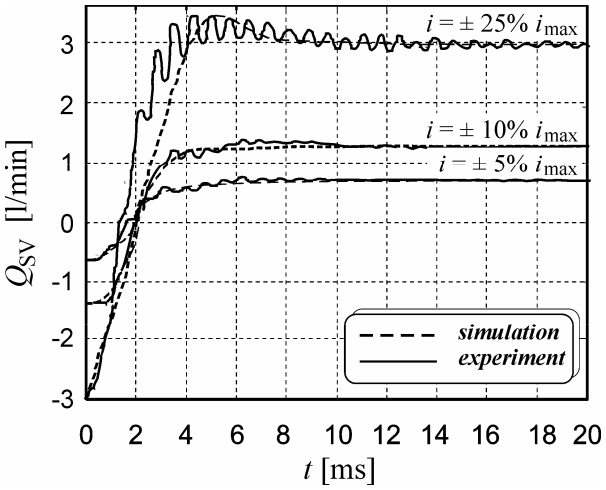

Fig. 9: *The transient response of the servovalve*

When current signals are ±5% or ±10% of the rated current, the coincidence between the experiment and the simulation is obvious. A slight discrepancy can be observed for the highest signal (±25% of i^*_{max}). There are several reasons for this phenomenon. The validity of experimental results is questionable. The equipment can hardly provide constant values of pressures in actuator chambers for this level of input signal due to considerable oscillations of actuator around its null position. It is also difficult to provide the ideal square current input signal for this input signal level. It is also worth mentioning that the numerical transient response is slightly slower because the flapper hits the nozzle and the Eq. 19, which describes this phenomenon, is intuitively presumed. In Eq. 10, this term influences several flapper impacts on the nozzle. This "shaky" movement slows down the servovalve transient response. It is doubtful if this really occurs or flapper sticks on the nozzle for a while after the impact.

Results of numerical and experimental static flow characteristics of the servovalve are comparatively presented in Fig. 10. The input current signal was the periodic sinusoidal signal which amplitude was i^*_{max} and the frequency 1/16 Hz. The figure shows good agreement of the experiment and the simulation. The hysteresis can be spotted in the numerically obtained curve. The hysteresis loop of the experimental curve is somehow wider because the torque motor hysteresis was not considered in the simulation.

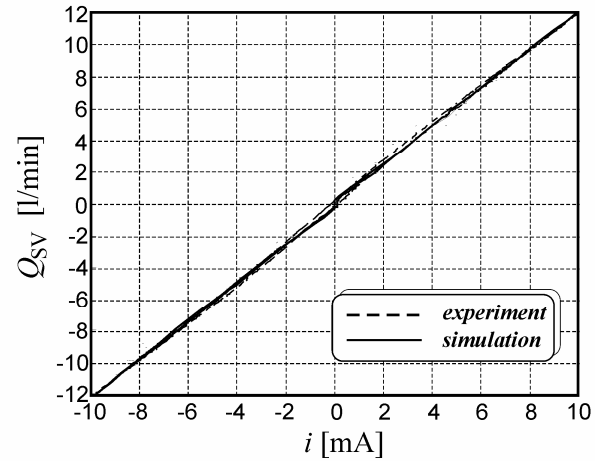

Fig. 10: *The static flow characteristic of the servovalve*

It could be concluded from the above, that the created mathematical model satisfactory describes behaviour of two-stage electrohydraulic servovalves with the spool position feedback, so it could be used for the servovalve analysis in many working regimes.

5 Conclusion

Using the extensive theoretical analysis (based on fundamental laws of fluid mechanics, electromagnetism and general mechanics, as well as experiences and results of the latest research), authors tried to create a conceptual servovalve mathematical model. This model includes phenomena and quantities of influence on analysed servovalve, so it can predict their performance in a wide range of expected working regimes. Its complexity is only limited by the possibility of correct numerical integration on a personal computer. The accuracy of the model was validated.

Such model primarily presents a useful design tool, since all its parameters are physical quantities. It could be also used as a fine base for the electrohydraulic servosystem design with the application of advanced control techniques.

The biggest improvement of the model would comprise finding a way for the precise measuring of spool and armature assembly friction coefficients.

Nomenclature

A_m	permanent magnet cross sectional area	[m^2]
A_p	torque motor gap area	[m^2]
A_s	spool side area	[m^2]
B_{fl}	flapper bending rigidity	[Nm^2]
B_t	flexure tube rigidity	[Nm^2]
d_n	nozzle diameter	[m]
d_o	left (right) constant orifice diameter	[m]
d_{od}	drain constant orifice diameter	[m]
d_s	spool diameter	[m]
e	spool eccentricity	[m]
f	spool valve area gradient	[m]
F_a	axial component of flow force on spool	[N]
F_c	dry friction force on spool	[N]
F_{c0}	initial dry friction force on spool	[N]
F_{cn}	nominal dry friction force on spool	[N]
F_f	force caused by mutual action of feedback spring and spool	[N]
F_h	flow force on flapper	[N]
H_i	length of i-th spool orifice	[m]
i^*	total current (parallel and series connection) or current difference in two coils (push-pull connection)	[A]
i_{max}	rate input current	[A]
i_s	electronic amplifier saturation	[A]
J_a	armature assembly moment of inertia with the respect of rotational centre	[kgm^2]
K_a	electronic amplifier signal gain	[A/V]
k_c	coil connection coefficient; k_c=1 for parallel, and k_c=2 for serial and push-pull coil connection	[-]
K_{ci}	contraction coefficient of i-th spool orifice	[-]
K_f	feedback spring stiffness	[N/m]
k_i	"impact stiffness"	[N/m]
K_i	torque motor gain	[Nm/A]
k_l	constant of leakage flux in air gap	[-]
k_m	constant caused by the non-uniformity of magnetic field in permanent magnet	[-]
K_m	torque motor electromagnetic spring constant	[Nm]
k_n	spool viscous friction coefficient	[kg/s]
K_{nl}	flow coefficient of the left flapper-nozzle restriction	[-]
K_{nr}	flow coefficient of the right flapper-nozzle restriction	[-]
K_{od}	flow coefficient of the drain constant orifice	[-]
K_{ol}	flow coefficient of the left constant orifice	[-]
K_{or}	flow coefficient of the right constant orifice	[-]
K_p	electrical feedback (including position transducer) gain	[V/m]
k_r	magnetic reluctance constant	[-]
K_{ti}	flow coefficient of i-th spool orifice	[-]
k_v	armature assembly viscous friction coefficient	[Nms]
l_1	axial length between supply port and actuator port	[m]
l_2	axial length between reservoir port and actuator port	[m]
l_a	distance from the nozzle axis of symmetry to the axis of rotation of armature assembly	[m]
l_f	feedback spring length	[m]
l_{fl}	flapper length	[m]
l_l	length of spool end lands	[m]
l_m	permanent magnet length	[m]
l_o	left (right) constant orifice length	[m]
l_{od}	drain constant orifice length	[m]
l_t	flexure tube length	[m]
M_m	permanent magnet magnetomotive force	[A]
m_s	spool mass	[kg]

N	number of turns of each coil	[-]
p_0	atmospheric (reservoir) pressure	[Pa]
p_d	drain orifice inlet pressure	[Pa]
p_l	left nozzle pressure	[Pa]
p_{L1}	pressure in right actuator chamber	[Pa]
p_{L2}	pressure in left actuator chamber	[Pa]
p_r	right nozzle pressure	[Pa]
p_s	supply pressure	[Pa]
r	distance from armature pivot to the centre of permanent magnet pole face	[m]
r_b	radius of bushing control edge	[m]
Re_{nl}	left flapper-nozzle restriction Reynolds number	[-]
Re_{nr}	right flapper-nozzle restriction Reynolds number	[-]
Re_{od}	drain constant orifice Reynolds number	[-]
Re_{ol}	left constant orifice Reynolds number	[-]
Re_{or}	right constant orifice Reynolds number	[-]
R_{mm}	permanent magnet reluctance	[H^{-1}]
R_{mp0}	reluctance of each air gap at the null	[H^{-1}]
r_s	radius of spool control edge	[m]
T_e	torque caused by electromagnetic forces	[Nm]
T_f	torque caused by feedback spring deformation	[Nm]
T_i	torque caused by flapper impact against nozzle	[Nm]
T_t	torque caused by flexure tube deformation	[Nm]
T_{tot}	total torque on armature	[Nm]
U	input voltage	[V]
V_d	drain compartment volume	[m^3]
V_l	enclosed volume on each spool when y=0	[m^3]
Q_{li}	leakage flow through i-th spool orifice	[m^3/s]
Q_{L1}	volumetric flow through the right actuator chamber	[m^3/s]
Q_{L2}	volumetric flow through the left actuator chamber	[m^3/s]
Q_{nl}	volumetric flow through the left nozzle	[m^3/s]
Q_{nr}	volumetric flow through the right nozzle	[m^3/s]
Q_{ol}	volumetric flow through the left constant orifice	[m^3/s]
Q_{or}	volumetric flow through the right constant orifice	[m^3/s]
Q_{od}	volumetric flow through the drain constant orifice	[m^3/s]
Q_{SV}	servovalve volumetric flow	[m^3/s]
Q_i	volumetric flow through i-th spool orifice	[m^3/s]
x	flapper tip displacement	[m]
x_0	distance from flapper tip to each nozzle at null	[m]
x_n	distance from flapper tip to nozzle	[m]
x_{p0}	length of each air gap at null	[m]
y	spool displacement	[m]
y_{0i}	null lap condition of i-th spool orifice	[m]
y_f	feedback spring end deflection	[m]
y_{ff}	fictive feedback spring ball displacement if there is no spool	[m]
y_i	i-th spool orifice opening	[m]
y_{tl}	large transition length	[m]
z	half the feedback spring ball clearance	[m]
Δp_i	pressure drop at i-th spool orifice	[Pa]
α_i	jet angle in i-th spool orifice	[°]
β	fluid compressibility	[Pa]
δ	spool in bushing radial clearance	[m]
η	fluid dynamic viscosity	[Pa·s]
φ	flapper free end inclination	[rad]
μ_0	magnetic permeability of vacuum	[H/m]
μ_m	permanent magnet permeability	[H/m]
ν	fluid kinematic viscosity	[m^2/s]
θ	armature deflection	[rad]
ρ	fluid density	[kg/m^3]

Acknowledgements

The support of PPT (Prva Petoletka – Trstenik) for this study is gratefully acknowledged.

References

Arafa, H.A and **Rizk, M.** 1987. Identification and Modelling of Some Electrohydraulic Servo-Valve Non-Linearities. *Proceedings of the Institution of Mechanical Engineers, Part C: Mechanical Engineering Science*, Vol. 201, No. 2, pp. 137-144.

Babić, M., Gordić, D. and **Šušteršič, V.** 2002. Determination of Values for Flow Coefficients of First Stage Orifices in Two-Stage Electrohydraulic Servovalves. *Proc. of the 4th Intern. conf. - Heavy machinery-HM'02*, Kraljevo, Serbia. pp. E13-E16.

Bergadà, J. and **Codina, E.** 1994. Discharge Coefficients for a Four Nozzle Two Flapper Servovalve. *Proc. of the 46th National Conference on Fluid Power*, Vol. 1, Anaheim, USA, pp. 213-218.

Burrows, C., Mu, C. and **Darling, J.** 1991. A Dynamic Analysis of a Nozzle-Flapper Valve With Integral Squeeze Film Damper. *ASME Journal of Dynamic Systems, Measurement and Control*, Vol. 113, No. 4, pp. 702-708.

Dong, X. and **Ueno, H.** 1999. Flows and Flow Characteristics of Spool Valve. *Proc.of the Forth JHPS International Symposium on Fluid Power* (Tokyo '99), *Japan, pp. 51-56.*

Ellman, A. 1998. Leakage Behaviour of Four-Way Servovalve. *Fluid Power Systems and Technology 1998, FPST Vol. 5, Collected papers of 1998 ASME IMECE*, Anaheim, USA, pp. 163-167.

Ellman, A. and **Virvalo, T.** 1996. Formation of Pressure Gain in Hydraulic Servovalves and Its Significance in System Behaviour. *Fluid Power Systems and Technology 1996, FPST Vol. 3,*

Collected papers of 1996 ASME IMECE, Atlanta, USA, pp. 77-81.

Eryilmaz, B. and **Wilson, B.** 2000. Modeling the Internal Leakage of Hydraulic Servovalves. *Proc. of the 2000 ASME International Mechanical Engineering Congress and Exposition*, Vol. DSC-69.1, Orlando, USA, pp. 337-343.

Gordić, D. 2002. *The Analyses of the Two-Stage Electrohydraulic Servovalves With the Spool Position Feedback.* PhD thesis, The University of Kragujevac, Kragujevac, Serbia (In Serbian)

Gordić, D., Jovičić, N., Šušteršič V. and **Živanović, J.** 2003. The Calculation of the Stationary Axial Flow Force on a Spool Valve. *Proceedings of the Fifth International Conference DEMI*, Banja Luka, Bosnia and Herzegovina, pp. 203-208.

Hayase, T., Hayashi, S. and **Kojima, K.** 1996. Micro Stick-Slip Vibration in Hydraulic Servo Systems. *Proc.of the Third JHPS International Symposium on Fluid Power* (Yokohama '96), Japan, pp. 555-560.

Karan, R., Scheidl, R. and **Aberl, H.** 1996. Modeling and Identification of Hydraulic Servo-Valves. *Proc. 1st European Conf. on Structural Control*, Vol. 13, Series B, Barcelona, Spain, pp. 121-129.

Lee, J.-C., Misawa, E. and **Reid, K.** 1996. Stability Robustness Applied to the Design of Electrohydraulic Servovalve. *Proceedings of IEEE Conference on Control Applications*, Dearborn, USA, 1996, pp. 534-539.

Lin, S. J. and **Akers, A.** 1991. Dynamic Analysis of an Flapper-Nozzle Valve. *ASME Journal of Dynamic Systems, Measurement and Control*, Vol. 113, No. 1. pp. 163-167.

McCloy, D. and **Martin, H. R.** 1973. *The Control of Fluid Power*. Longman Group LTD, London.

Merritt, H. 1967. *Hydraulic Control Systems*. John Wiley & Sonse, New York.

van Schothorst, G. 1997. *Modeling of Long-Stroke Hydraulic Servo-Systems for Flight Simulator Motion Control and System Design.* PhD thesis, Tehnische Universiteit Delft, Netherlands.

Shearer, J. L. 1980. The Effects of Radial Clearance, - Rounded Corners, and Underlap on Servovalve Characteristics. *Proceedings of Joint Automatic Control Conference*, Vol. 1, San Francisco, USA, paper TA9-G.

Southward, S. C., Radcliffe, C. J. and **MacCluer, C. R.** 1991. Robust Nonlinear Stick-Slip Friction Compensation. *ASME Journal of Dynamic Systems, Measurement, and Control*, Vol. 113, December, pp. 639-644.

Svensson, B. 1993. *Simulation of an Electrohydraulic Servovalve*. LiTH-IKP-Ex-1092, UK.

Tawfik, M. 1999. *Model Based Control of an Electro-Hydraulic Servovalve*. PhD thesis, University of Akron, Ohio, USA.

Thayer, W. J. 1965. *Transfer Functions for Moog Servovalves*. Moog Technical Biletin 103, East Aurora, NY, USA.

Urata, E. 1999. Dynamics of Elastic Structure in Servovalve Torque Motors. *Bath Workshop on Power Transmission and Control (PTMC'99)*, Bath, UK, pp. 183-196.

Urata, E. 2000. Study of Magnetic Circuits for Servovalve Torque Motors. *Bath Workshop on Power Transmission and Control (PTMC'00)*, Bath, UK, pp. 269-282.

Urata, E. and **Shinoda M.** 1999. Influence of Amplifier and Feedback on the Dynamics of a Water Hydraulic Servovalve. *Proc.of the Forth JHPS International Symposium on Fluid Power* (Tokyo '99), Japan, pp. 567-572.

Vilenius, M. J. and **Vivaldo, T. K.** 1976. The Effect of Nonlinearities on the Dynamic Characteristics of an Electrohydraulic Servovalve. *Hydraulic and Pneumatic, Mechanical Power*, Vol. 22, No. 263, pp. 419-424.

Wang, D., Dolid, R., Donath, M. and **Albright, J.** 1995. Development and Verification of a Two-Stage Flow Control Servovalve Model. *American Society of Mechanical Engineers. The Fluid Power and Systems Technology Division (Publication), FPST*, Vol. 2, pp. 121-129.

Watton, J. 1989. *Fluid Power System: Modeling, Simulation, Analogue and Microcomputer Control.* Prentice Hall, New York.

van Wel, O. P. 1992. *The Modeling of an Electrohydraulic Servovalve*. Master thesis, Delft University of Technology, Mechanical Engineering System and Control Group, Netherlands.

Yeaple, F. 1996. *Fluid Power Design Handbook*. Third Edition, Marcell Dekker, New York.

Dušan Gordić
Born in Prijepolje, Serbia in 1970. PhD in Mechanical Engineering from the University of Kragujevac in 2002. Assistant professor in the area of Fluid power & control at the Faculty of Mechanical Engineering in Kragujevac. He works on CAD of fluid power devices and applications of multimedia in fluid power lecturing.

Milun Babić
Born in Sjenica, Serbia in 1951. PhD in Mechanical Engineering from the University of Belgrade in 1982. Professor of Hydraulic & pneumatic machinery at the Faculty of Mechanical Engineering in Kragujevac. He was a leader in many R&D projects performed at the Faculty concerning hydraulic machineries, hydrodynamic couplings and process plants. Presently working on energy efficiency.

Nebojša Jovičić
Born in Kragujevac, Serbia in 1963. PhD in Mechanical Engineering from the University of Kragujevac in 2000. Assistant professor in the area of Numerical methods and CFD at the Faculty of Mechanical Engineering in Kragujevac. Current research on new solutions for wind turbine design